

## Research Article

# Vegetable Oil and Derivates Hydroprocessing Using Ni as Catalyst for the Production of Hydrocarbons

Lívia C. T. Andrade <sup>1</sup>, Germildo J. Muchave,<sup>1</sup> Samia T. A. Maciel,<sup>2</sup> Isabelly P. da Silva,<sup>3</sup> Gabriel F. da Silva,<sup>4</sup> João M. A. R. Almeida,<sup>5</sup> and Donato A. G. Aranda<sup>1</sup>

<sup>1</sup>Programa de Pós-Graduação em Engenharia de Processos Químicos e Bioquímicos (E.P.Q.P.)-Escola de Química, Universidade Federal Rio de Janeiro (UFRJ), Av. Athos da Silveira No. 149, Centro de Tecnologia Bloco E, 21941-909 Rio de Janeiro-RJ, Brazil

<sup>2</sup>Sergipe Parque Tecnológico, Rodovia João Bebe Água, No. 731, 49100-000 São Cristóvão-SE, Brazil

<sup>3</sup>Departamento de Engenharia de Produção, Universidade Federal de Sergipe (UFS), Av. Marechal Rondon n/No., 49100-000 São Cristóvão-SE, Brazil

<sup>4</sup>Laboratório de Tecnologias Alternativas (L.T.A), Universidade Federal de Sergipe (UFS), Av. Marechal Rondon n/No., 49100-000 São Cristóvão-SE, Brazil

<sup>5</sup>Instituto de Química (I.Q.), Universidade Federal do Rio de Janeiro (UFRJ), Av. Athos da Silveira Ramos No. 149, Centro de Tecnologia Bloco A 5° Andar, 21941-909 Rio de Janeiro-RJ, Brazil

Correspondence should be addressed to Lívia C. T. Andrade; [livia.adr@eq.ufrj.br](mailto:livia.adr@eq.ufrj.br)

Received 29 October 2021; Revised 8 January 2022; Accepted 24 February 2022; Published 24 March 2022

Academic Editor: Mulugeta Admasu Delele

Copyright © 2022 Lívia C. T. Andrade et al. This is an open access article distributed under the Creative Commons Attribution License, which permits unrestricted use, distribution, and reproduction in any medium, provided the original work is properly cited.

The aviation sector has become a considerable market for biofuels since they come from renewable sources and have characteristics that help to reduce pollution. Hydrocarbons production from vegetable oils and their derivates for use in diesel and aviation kerosene are a possible alternative route to reduce fossil fuels. With that in mind, this article aimed to develop nickel catalysts supported on  $\gamma$ -Al<sub>2</sub>O<sub>3</sub>, Nb<sub>2</sub>O<sub>5</sub>, and zeolites to submit them to the hydroprocessing of vegetable oils and derivatives in the production of hydrocarbons. With soy ester, reactions with the Ni/Al<sub>2</sub>O<sub>3</sub> and Ni/Nb<sub>2</sub>O<sub>5</sub> catalyst showed selectivity of 41.2 and 16.5%, respectively, at a temperature of 300°C and a reaction time of 7 h. Under the same conditions, hydroprocessing reactions for the soybean ester using Ni/Beta and Ni/HY zeolites promoted more excellent conversion (between 80 and 99%) than oxide catalysts and selectivity between 30 and 70% for Ni/Beta and Ni/HY, correspondently. Besides, zeolite catalysts showed high conversion at the higher temperature (340°C) and time (9 h), reaching 100% conversion and hydrocarbons selectivity of 76.8 and 61.9% for zeolite Beta and HY, respectively. Changing the raw material to fatty acids made it possible to notice that zeolite catalysts showed high selectivity reaching 100%. Given the excellent performance of catalysts in hydroprocessing reactions, it is possible to consider them a promising alternative route since they can reduce the production by applying transition metal as a catalyst instead of noble metals used in the industry.

## 1. Introduction

There are several reasons for the growing use of renewable hydrocarbons, including the need to reduce greenhouse gas emissions (GHG). According to IPCC (Intergovernmental Panel on Climate Change), air traffic reaches global emissions between 2 and 3% per year. National Civil Aviation Agency (ANAC) predicts that, in the coming years, air traffic

will double, consequently reaching 5-6% of the global GHG by 2050 [1]. The IATA (International Air Transport Association) has set ambitious targets for its associates, including the absolute reduction of 50% in the sector emissions by 2050, compared to 2005 [2].

Sustainability is an essential element in the face of public acceptance of any alternative fuel. Therefore, the best option is advanced biofuels obtained from innovative technologies

and sustainable crops or agricultural coproducts [3]. Thus, the use of aviation biokerosene (biojet fuel) has been studied and applied in adequate mixtures with fossil kerosene [4].

Due to the growing demand for fuels and the consequent concern with the problems related to the burning of these products, there is an interest in developing new technologies linked to natural resources to generate renewable energy, replacing conventional sources. Biomass is an excellent alternative for biofuels production [5].

Diesel and biokerosene alkanes have received greater attention in the last decade ranging from the catalytic hydroprocessing of fatty acids or esters derived from biomass oils (vegetable oils, animal fats, and residual oils). Commonly, these oils contain fatty acids between C14 and C24, with a predominance of C18, presenting fuel properties similar to petroleum derivatives, suitable for producing hydrocarbons [6].

The palm is one of the most productive oil seeds. Some varieties even produce 10 tons of oil per hectare per year (20 times more than soybeans). From this oilseed, nonlauric oil can be extracted, found in the fibrous pulp surrounding the fruit seed, rich in carotenoids (Beta-carotene), and has significant antioxidants and lauric oil present in almonds. Compared to other vegetable oils, palm oil consumes less hydrogen during hydroprocessing, as it contains a smaller fraction of unsaturated fatty acids in the composition [7]. Studies show that the hydroprocessing of fatty acids to produce hydrocarbons in the diesel range is more efficient than triglycerides. The fatty acid compositions are mainly free fatty acids (palmitic, oleic, and linoleic), more easily converted to aliphatic alkanes than triglycerides [8]. There is a need for an in-depth and detailed study of vegetable oils, particularly to identify how they can be hydroprocessed, assuming that there is already an infrastructure refinery for raw materials derived from petroleum, such as diesel. To maximize the reagent conversion, some authors use technologies to convert lipid raw materials into distilled fuels [9].

It is possible to convert vegetable oils into liquid alkanes through hydroprocessing. The reaction involves hydrogenating the vegetable oil's double bonds transformed into monoglycerides, diglycerides, and carboxylic acids [10]. These intermediate products are converted to alkanes by three different routes: decarboxylation, decarbonylation, and hydrogenation/dehydration [11]. Straight chain alkanes (C15-C18) can undergo isomerization and cracking to produce more light and isomerized alkanes. In comparison, the fatty acids obtained in the hydrotreating process can catalyze isomerization and cracking reactions. Besides, wax esters can convert to hydrocarbons (Figure 1).

By analyzing the reaction scheme of the transformation of fatty acid methyl esters (FAME) into hydrocarbons, it is possible to verify that the hydrogenation occurs first and then the hydrodeoxygenation [6]. High operating conditions are required to achieve more excellent conversion of reactants to hydrocarbons from triglycerides. More C17 hydrocarbons are obtainable due to the decarbonylation/decarboxylation reaction [12].

Based on the reaction scheme shown in Figure 2, it is also possible to convert esters to hydrocarbons through

hydroprocessing. The process begins with the ester's hydrogenation, the products of this reaction being fatty alcohol and methanol. The fatty alcohol (an intermediate product) reacts with the ester to form a hydrogenated wax and can produce two fatty alcohols undergoing dehydration and hydrogenation to form hydrocarbons.

According to the literature, the hydroprocessing reaction of esters and fatty acids (HEFA) presents several advantages over other techniques, such as the method's similarity with traditional refineries and lower cost [13, 14]. The hydroprocessing route is one of the most promising routes for hydrocarbon production, since it can be used in existing refineries, producing hydrocarbons similar to those of fossil origin, which can be used in internal combustion engines and turbine engines without the need for changes [15, 16]. This type of fuel is called drop-in fuel [17].

However, the available technologies still need to be improved to obtain hydrocarbons at commercially competitive costs. Therefore, the development of catalysts is necessary to improve conversion and selectivity. The catalysts allow the reaction to be carried out under lower temperature and pressure conditions, which will help reduce operating costs [18].

Many heterogeneous catalysts have been reported in the literature, being used in numerous reactions, including oxides, mixed oxides, zeolites, clays, resins, and mesoporous solids. According to Chen et al. [6], producing hydrocarbons from hydroprocessing requires the application of heterogeneous catalysts, which must present simultaneous hydrogenation and cracking characteristics. The first main catalysts presented in the literature with excellent yield are catalysts based on noble metals (platinum, palladium, and rhenium), generally supported by zeolites or oxides. Although noble metal catalysts are more stable resisting rapid deactivation and have more excellent catalytic activity. They are not viable for application in a large-scale process due to the high acquisition cost [19].

Catalysts based on transition metals such as nickel, copper, molybdenum, cobalt, tungsten, and iron or their bimetallic composites supported, in most cases, by alumina ( $\text{Al}_2\text{O}_3$ ) or niobium ( $\text{Nb}_2\text{O}_5$ ), generally present high conversion in hydroprocessing; however, the sulfur leaching contained in some raw materials can contaminate the products [20, 21]. Due to the high cost of noble metal catalysts and the possible contamination by sulfur (S) of the final product when using sulfide catalysts, there has been increased research in recent years to develop low-cost catalysts. Selecting the most suitable catalysts in terms of conversion, selectivity, stability, and valuable life increases the process's economic viability and sustainability as a whole [22]. Catalysts supported on niobium, alumina, and zeolites have been widely reported in the literature in hydrolysis, hydroesterification, and hydroprocessing reactions, presenting satisfactory results [18].

Considering the relevance of increasing the use of renewable fuels, the objective of this study was to develop a new catalytic system that can guarantee the efficient production of hydrocarbons allowing a new way of processing less polluting fuels, which until now have not been addressed

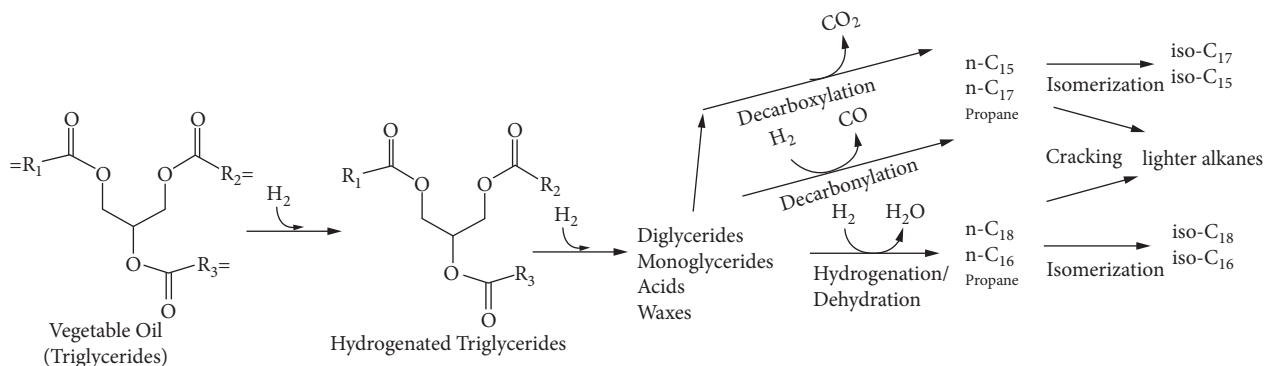
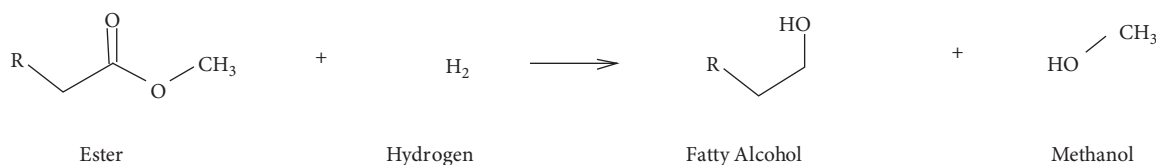
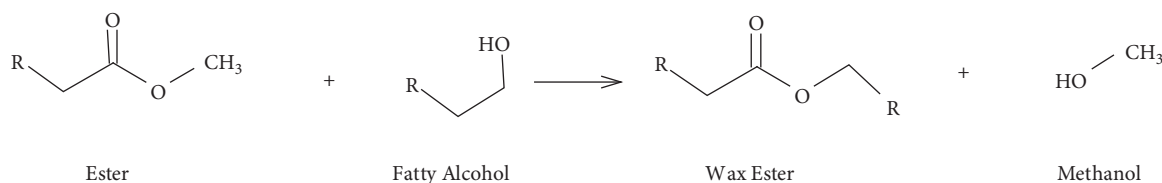


FIGURE 1: Reaction scheme for converting triglycerides to hydrocarbons. Source: Huber et al. [10].

Stage 1



Stage 2



Stage 3

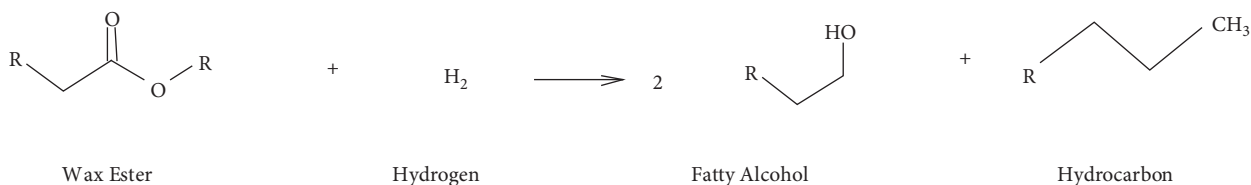


FIGURE 2: Reaction scheme for the conversion of esters to hydrocarbons.

in the literature, from renewable raw materials (derived from vegetable oils, methyl esters, and fatty acids), by catalytic hydroprocessing using nickel catalysts supported on oxides (Al<sub>2</sub>O<sub>3</sub> and Nb<sub>2</sub>O<sub>5</sub>) and zeolites (Beta and HY), evaluating the temperature influence, time, and types of catalysts in producing hydrocarbons (conversion and selectivity).

## 2. Materials and Methods

The experiments were conducted in a bench scale at Laboratório de Tecnologias Verdes (GREENTEC), at Escola de Química-UFRJ.

**2.1. Materials.** The tests were conducted with commercial palm oil (provided by Agropalma) because it contains a more significant amount of saturated C16 and C18 (palmitic and stearic) in its composition, which influences the carbon chain in hydrogenation, soybean methyl ester for having more C18 unsaturated fatty acids (oleic and linoleic) to evaluate the formation of isomers, and soybean fatty acid (provided by Granol) as feedstocks for hydroprocessing, using monometallic alumina-based nickel catalysts (γ-Al<sub>2</sub>O<sub>3</sub>) supplied by SASOL and Niobia (Nb<sub>2</sub>O<sub>5</sub>), provided by CBMM, Brazilian Company of Metallurgy and Mining and, subsequently, hydrogen 99.99% (Line Gases), nickel

nitrate 99.99% [Ni(NiO<sub>3</sub>)<sub>2</sub>] (Sigma-Aldrich), catalysts based on Beta, and HY zeolites provided by Unidade Protótipo de Catalisadores, PROCAT/UFRJ.

**2.2. Catalyst Synthesis.** Synthesis of the alumina- and Niobia-supported incipient wetness impregnation catalysts following previous methods is described in the literature [12, 23, 24]. The supports were dried at 100°C overnight. Then nickel nitrate [Ni(NiO<sub>3</sub>)<sub>2</sub>] was dissolved in distilled H<sub>2</sub>O and after this solution was added dropwise to 10 g of the support. The reaction mixture was oven-dried at 100°C for 12 hours. Subsequently, the catalysts were calcined in a muffle furnace at 600 (Ni/Al<sub>2</sub>O<sub>3</sub>) and 400°C (Ni/Nb<sub>2</sub>O<sub>5</sub>) for 4 hours. It is essential to mention that the calcination temperature was 400°C for the Ni/Nb<sub>2</sub>O<sub>5</sub> catalyst to evaluate the results while maintaining the amorphous structure of Niobia. The impregnated metal (Ni) proportion at the supports was 15% (wt/wt). Nickel catalysts based on Beta and HY zeolites were synthesized by the incipient wetness impregnation method in Unidade Protótipo de Catalisadores, PROCAT/UFRJ. The goal was to obtain 15% nickel (wt/wt) in all catalysts.

**2.3. Catalyst Characterization.** The materials were characterized by nitrogen physisorption techniques, which determined textural properties (surface area, volume, and pore diameter). Analyses were performed on the Micromeritics A.S.A.P. 2020. Before analysis, the samples were pretreated at 300°C overnight under vacuum. The X-ray diffraction (XRD) technique was used to identify the crystalline structures that make up the catalysts and possible modifications after impregnation, using a Rigaku diffractometer, model Miniflex II, with a monochromator and Cu radiation under angular scanning from 5 to 90° with an increment of 0.05° and counting time of 1 s/step. X-ray fluorescence (XRF) was applied to identify and quantify the chemical composition of the catalysts and used Rigaku equipment of model Primini. A tablet containing 5 g of sample was prepared using the quantitative and qualitative oxide method to analyze. Temperature Programmed Reduction (TPR) was performed to determine the catalyst's reduction temperature, using a Micromeritics Autochem TPR-2920 Crycooler II model. Before the experiments, the catalysts were pretreated at 150°C at an argon (Ar) flow rate of 30 ml/min. The reduction was conducted in an H<sub>2</sub>/Ar flow rate of 30 ml/min until 1000°C. Temperature program desorption of ammonia (NH<sub>3</sub>-TPD) was used to determine the strength of the acid. NH<sub>3</sub>-TPD experiments were carried out in an instrument equipped with a thermal conductivity detector (TCD). For each run, 150 mg catalyst under 5 vol% H<sub>2</sub>/N<sub>2</sub> flow was packed into the U-type quartz tube reactor and pretreated in a flow of nitrogen (30 mL/min) at 150°C for 30 min. Then, the sample was cooled to 70°C for adsorbed ammonia until the saturated state and the physically adsorbed ammonia were removed by purging helium at the same temperature. The NH<sub>3</sub>-TPD profile was recorded by programming the temperature from 30 to 800°C, with a heating rate of 20°C/

min. The infrared spectroscopy with Fourier transformation (FTIR) of adsorbed pyridine was performed to determine the acidic sites' nature (Lewis and Brønsted). FTIR was carried out in a Shimadzu IRPrestige-21 equipment. For pyridine adsorption, 0.1 g of each calcined sample was deposited in a container containing 1 mL of pyridine in the liquid phase. The recipient was closed and manually shaken. After 24 h, excess of pyridine was evaporated at 100°C for 3 h; dried samples were analyzed with FTIR in the range of 1400–1580 cm<sup>-1</sup>, resolution of 2 cm<sup>-1</sup>, and 16 scans. The background was done with the calcined samples without pyridine adsorption [25].

**2.4. Catalytic Tests.** The catalysts were reduced in a reactor with hydrogen at a reduction temperature of 450, 400, 425, and 550°C for Ni/Al<sub>2</sub>O<sub>3</sub>, Ni/Nb<sub>2</sub>O<sub>5</sub>, Ni/HY, and Ni/Beta, respectively, for 4 hours and heating ramp of 5°C/min. Catalytic hydrogenation was conducted in a Parr reactor model 4848 with a maximum capacity of 300 mL, maximum pressure of 3000 psi, temperature control system pressure, and automatic agitation of 1200 rpm; solvent was not used to perform the reactions.

The parameters studied to evaluate the conversion and selectivity of Ni/Al<sub>2</sub>O<sub>3</sub> and Ni/Nb<sub>2</sub>O<sub>5</sub> catalysts were reaction time (5 and 7 hours), temperature (270, 290, and 300°C), constant pressure of 70 bar, flow H<sub>2</sub> during hydrotreating as semibatch operation, and 3% (w/w) of catalyst. From the results obtained, zeolites (Beta and HY) were applied to compare and analyze the increased conversion and selectivity, in addition to observing isomerization along with hydrogenation, starting the tests in the best temperature condition (300°C) and then rising to 340°C. Additionally, the reaction time was increased to 9 hours to increase conversion and selectivity.

**2.5. Gas Chromatographic (GC) Analysis.** The identification and quantification of hydrocarbons were carried out using the ASTM D6584 international standard methodology. Chromatographic analysis was performed on the gas chromatograph (Shimadzu, model GC-2010), with split/splitless injector, flame ionization detector FID, and DB23 column (0.32 mm ID).

### 3. Results and Discussion

#### 3.1. Catalyst Characterization

**3.1.1. Textural Properties (BET).** Textural analysis of the catalysts was performed to determine the surface area, the specific pore diameter, and pore volume, as shown in Table 1.

Table 1 shows that the zeolite catalysts have mesopores and micropores. Already the oxide-based catalysts (alumina and Niobia) have only mesopores in their structures. It was seen that, after the impregnation of metal, there was a reduction in the surface area accompanied by a decrease in pore volume. The increased catalyst density can explain this decrease due to the incorporation of metals in pores or the blocking of the pores caused by NiO agglomerates, which

TABLE 1: Textural properties of the catalysts and supports.

Catalyst	Surface area (BET) (m <sup>2</sup> /g)	Pore volume (cm <sup>3</sup> /g)	Pore size (Å)
Al <sub>2</sub> O <sub>3</sub>	222	0.45 (mesopores)	78
Ni/Al <sub>2</sub> O <sub>3</sub>	152	0.37 (mesopores)	91
Nb <sub>2</sub> O <sub>5</sub>	207	0.30 (mesopores)	59
Ni/Nb <sub>2</sub> O <sub>5</sub>	105	0.14 (mesopores)	52
Beta	511	0.71 (mesopores)	152
Ni/Beta	373	0.16 (micropores)	42
HY	708	0.33 (mesopores)	35
Ni/HY	534	0.12 (micropores)	25
		0.08 (mesopores)	
		0.27 (micropores)	
		0.11 (mesopores)	
		0.21 (micropores)	

reduces the adsorption capacity of the supports [12]. The increase in pore diameter of the Ni/Al<sub>2</sub>O<sub>3</sub> catalyst compared to the support can be explained by adsorption of the metal in internal pores and the surface of the alumina, thus increasing the particle size. Consequently, there was a decrease in surface tension due to the reduction in the contact area between the particles, increasing the pore diameter.

Similar results were reported by Gousi et al. [26] in which nickel supported on alumina, with different proportions of metal (10, 20, 30, 40, 60, 80, and 100%), was used as the catalyst. The metal's addition caused a slight reduction in the catalyst surface area, keeping this area relatively high even for higher nickel loads (up to 60% wt). Studies have shown that Niobia catalysts prepared with a low content of metals, such as platinum and gold, do not show relevant changes in the surface area and pore volume compared to pure support, presenting only a small reduction in the surface area and a slight increase in the pore diameter [27, 28].

Catalysts supported on zeolites showed a higher surface area than catalysts supported on metal oxides (alumina and Niobia). Similar results have been reported in the literature on the textural properties of catalysts supported by zeolites [29, 30]. For example, the HY support has a large surface area (708 m<sup>2</sup>/g), and, after nickel impregnation, there is a reduction in this area (534 m<sup>2</sup>/g), justified by a possible pore blockage [9]. Similar results were also obtained about the Ni/Beta catalyst and it was found that the support's surface area was 554 m<sup>2</sup>/g, and, after metal impregnation (5% Ni), there was a reduction to 511 m<sup>2</sup>/g. It was also found that as the metal content in the support increases, the area gradually decreases [20].

**3.1.2. X-Ray Diffractograms (XRDs).** Figure 3 illustrates the X-ray diffractograms (XRDs) of the Al<sub>2</sub>O<sub>3</sub> and Nb<sub>2</sub>O<sub>5</sub> (fresh material), Ni/Al<sub>2</sub>O<sub>3</sub>, and Ni/Nb<sub>2</sub>O<sub>5</sub> catalysts (after calcination) resulting from metal impregnation in the support by the wet spot impregnation method using nickel nitrate as a precursor.

XRD results of catalysts supported by oxides (Niobia and alumina) showed a structure similar to the structure of their supports, Al<sub>2</sub>O<sub>3</sub>  $2\theta = 37.3^\circ$  (311),  $46.0^\circ$  (400), and  $66.9^\circ$  (440), as well as Nb<sub>2</sub>O<sub>5</sub>  $2\theta = 26.3^\circ$  and  $53.0^\circ$ , as shown in Figure 3. As for the Ni/Al<sub>2</sub>O<sub>3</sub> catalyst (Figure 3(a)), besides the amorphous structure of the support, bands corresponding to nickel appeared at  $37.4^\circ$  (111),  $43.5^\circ$  (200),  $62.9^\circ$  (220),  $75.6^\circ$

(311), and  $79.8^\circ$  (222). Studies on the impregnation of metals in alumina reported the presence of the same structure [27]. The XRD performed for the Ni/Nb<sub>2</sub>O<sub>5</sub> catalyst (Figure 3(b)) showed that the support (Nb<sub>2</sub>O<sub>5</sub>) presented an amorphous structure, with no changes in the support structure after impregnation, indicating that the addition of nickel and subsequent heat treatment did not substantially alter the amorphous form of Niobia [31].

Figure 4 shows the diffractograms of the catalysts based on Beta and HY zeolites. The two catalysts have crystalline structures. Was observed the presence of peaks corresponding to nickel, identified with planes in the diffractograms, which appear at  $36.7^\circ$  (111),  $42.8^\circ$  (200),  $62.3^\circ$  (220),  $74.7^\circ$  (311), and  $78.9^\circ$  (222) for Ni/Beta (Figure 4(a)) and at  $37.8^\circ$  (111),  $44.0^\circ$  (200),  $63.6^\circ$  (220),  $70.6^\circ$  (311), and  $75.9^\circ$  (222) for Ni/HY (Figure 4(b)). The diffractograms of nickel oxide (NiO) and the referred supports presented in this work are similar to those reported in the literature [32]. According to the literature, although the diffraction intensity decreases with the Ni content, the catalyst structure does not significantly change. Chen et al. [20] identified some new diffraction peaks at  $2\theta$  of  $37.2^\circ$  (111),  $43.2^\circ$  (200), and  $62.8^\circ$  (220) due to the uniform dispersion of NiO particles on the support surface and as the Ni content was increased (5 to 15%), the characteristic peaks of NiO and Ni diffraction became increasingly accentuated in the diffractograms of the referred study.

**3.1.3. X-Ray Fluorescence (XRF).** From the results obtained through the XRF analysis, the oxide mass percentages of each sample are presented in Table 2.

The XRF results analysis indicates that the components already predicted in the composition of the catalysts (Ni/Al<sub>2</sub>O<sub>3</sub>, Ni/Nb<sub>2</sub>O<sub>5</sub>, Ni/Beta, and Ni/HY) result from their respective precursors during their impregnation. Although the predicted compositions were obtained, there is a difference between the theoretical value of 15% and the obtained values. It is possible to verify a slight reduction in the value obtained for the catalyst Ni/Nb<sub>2</sub>O<sub>5</sub> (12.5%) and the catalyst Ni/Al<sub>2</sub>O<sub>3</sub> (22.1%). According to the results provided by Priece et al. [33] and Horáček et al. [34], some surface concentrations may exceed the global values determined by XRF. Probably the metal became more dispersed in the surface layer, which may have caused this increase.

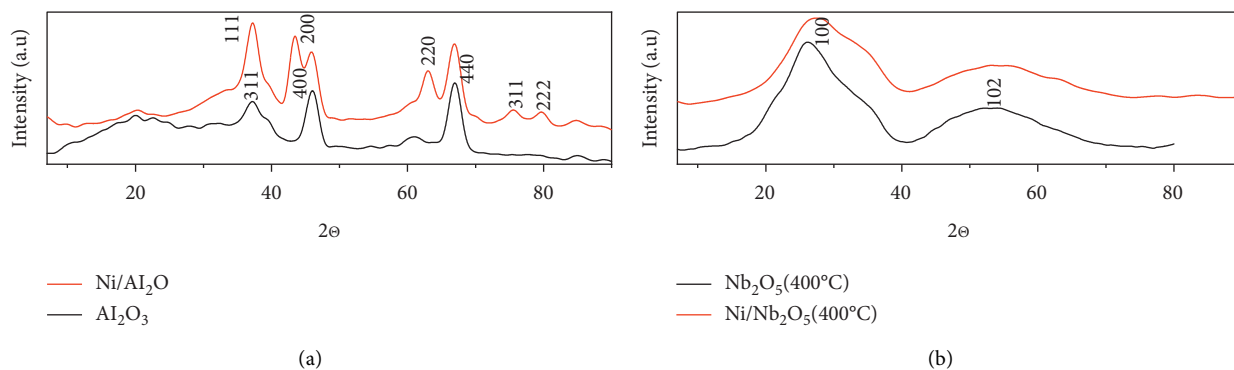


FIGURE 3: X-ray diffractogram of  $\text{Al}_2\text{O}_3$  and  $\text{Nb}_2\text{O}_5$ ,  $\text{Ni}/\text{Al}_2\text{O}_3$ , and  $\text{Ni}/\text{Nb}_2\text{O}_5$  catalysts.

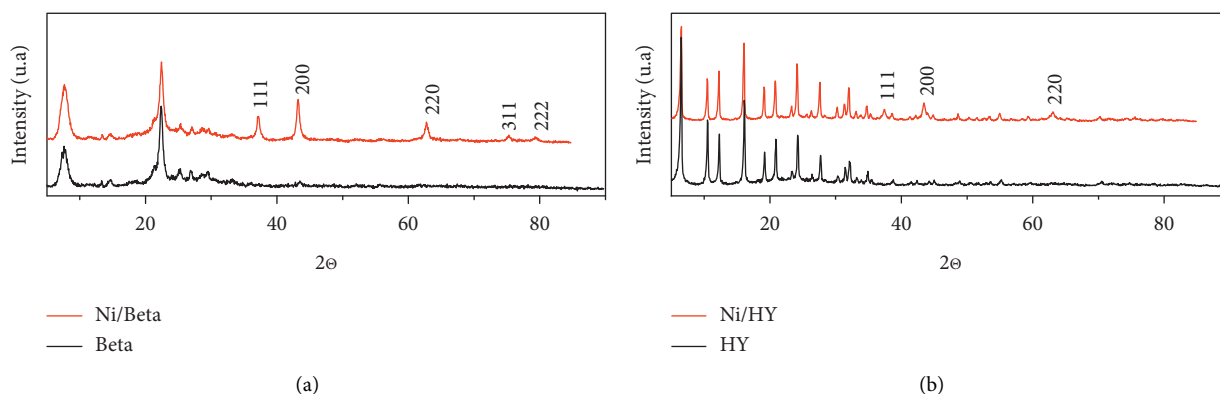


FIGURE 4: X-ray diffractogram of Beta HY,  $\text{Ni}/\text{Beta}$ , and  $\text{Ni}/\text{HY}$  catalysts.

Moreover, the differences between the theoretically predicted quantities and the obtained quantities can be attributed to experimental error.

**3.1.4. Temperature Programmed Reduction (TPR).** TPR analyses were performed to identify the appropriate temperatures for catalyst reduction. The results of the analysis of the catalysts are illustrated in Figure 5.

According to Figure 5, all catalysts have nickel reduction peaks. TPR profile of  $\text{Ni}/\text{Al}_2\text{O}_3$  catalyst (Figure 5 (a)) showed three peaks at 460, 600, and 900°C. The peak at 460°C was attributed to NiO weakly interacting with support. At 600 and 900°C, there were reductions in compounds with distinct NiO- $\text{Al}_2\text{O}_3$  interactions. The second peak at 600°C was attributed to NiO species interacting strongly with the support. Additionally, the peak reduction at high temperatures (at about 900°C) can be attributed to the nickel aluminate ( $\text{NiAl}_2\text{O}_4$ ) phase with spinel structure [23, 35]. TPR profile of  $\text{Ni}/\text{Nb}_2\text{O}_5$  catalyst (Figure 5 (b)) showed two peaks at 476 and 922°C. The peak at 476°C suggests a more significant interaction of Ni with the  $\text{Nb}_2\text{O}_5$  support occurrence (SMSI) and can be attributed to the reduction of  $\text{Ni}^{2+}$  to  $\text{Ni}^0$  [23, 36]. However, the second peak (at 922°C) related to the partial reduction of  $\text{Nb}_2\text{O}_5$  to  $\text{NbO}_2$  indicates interaction between Ni and  $\text{NbO}_5$  phases [36].

TABLE 2: Chemical composition of the prepared catalysts (wt% after impregnation).

Composition	$\text{Ni}/\text{Al}_2\text{O}_3$ (%)	$\text{Ni}/\text{Nb}_2\text{O}_5$ (%)	$\text{Ni}/\text{Beta}$ (%)	$\text{Ni}/\text{HY}$ (%)
Ni	22.1	12.5	15.7	14.9
$\text{Al}_2\text{O}_3$	77.9	—	8.1	13.7
$\text{Nb}_2\text{O}_5$	—	87.5	—	—
$\text{SiO}_2$	—	—	76.2	71.4

Two temperatures, 433 and 630°C, were observed in the  $\text{Ni}/\text{Beta}$  catalyst (Figure 5 (c)). The TPR plots showed greater intensity at lower temperatures. However, at higher reduction temperatures, they obtained the best results.  $\text{Ni}/\text{HY}$  catalyst (Figure 5 (d)) showed two or more reduction peaks with a higher incidence at 422°C and a peak at 589°C, commonly called shoulders in a work of catalytic deoxygenation of methyl laurate [37]; among the catalysts tested, the HY had a strong nickel in zeolites interaction. The highest reduction peak at 588°C was identified with NiO, and a peak at 355°C referred to free NiO.

**3.1.5. Temperature Programmed Desorption (TPD).** The deconvolution areas values and the temperature ranges in which the ammonia desorption occurred are shown in Table 3. According to the literature, catalysts can have three types of surface acidity classified as weak (<270°C), medium

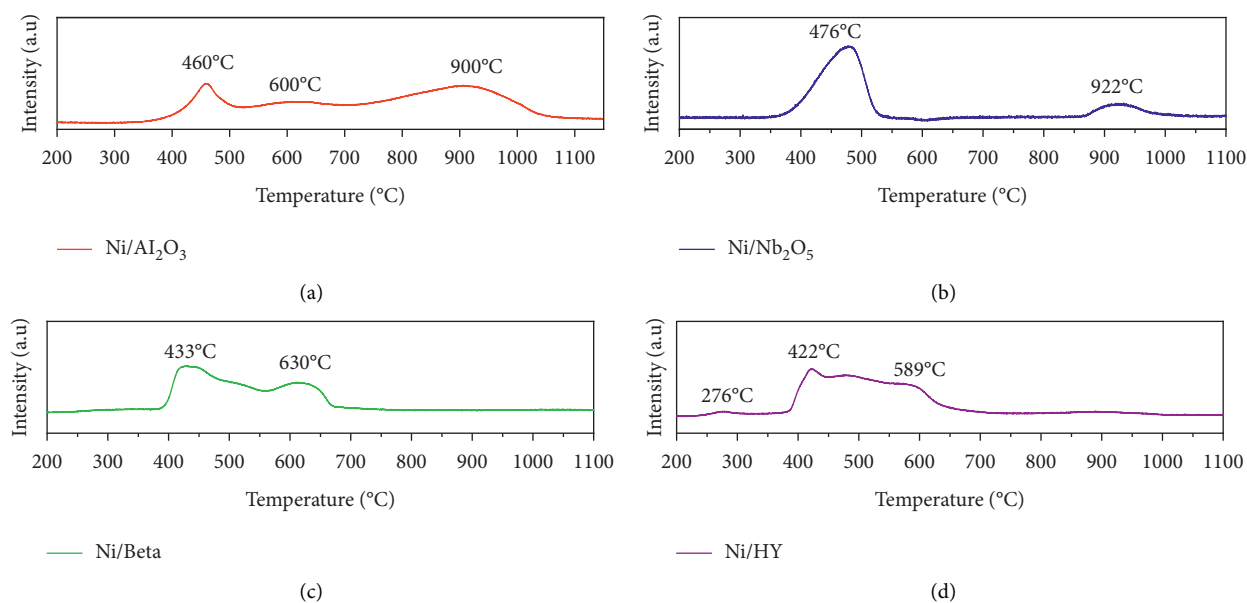


FIGURE 5: TPR profile of the Ni/Al<sub>2</sub>O<sub>3</sub>, Ni/Nb<sub>2</sub>O<sub>5</sub>, Ni/Beta, and Ni/HY catalysts.

(270–350°C), and strong (>350°C) based on ammonia desorption temperature [25, 38].

The NH<sub>3</sub>-TPD profiles of Ni/Al<sub>2</sub>O<sub>3</sub>, Ni/Nb<sub>2</sub>O<sub>5</sub>, Ni/Beta, and Ni/HY catalysts are shown in Figure 6. The Ni/Al<sub>2</sub>O<sub>3</sub> catalyst (Figure 6(a)) presented the profile displaced to higher temperatures, compared to the other catalysts (Ni/Nb<sub>2</sub>O<sub>5</sub>, Ni/Beta, and Ni/HY), with two different peaks at 315 and 515°C, respectively, with the first peak being attributed to weak acidic sites and the second to strong acidic sites [24, 26]. The other Ni/Nb<sub>2</sub>O<sub>5</sub>, Ni/Beta, and Ni/HY catalysts (Figures 6(b)–(d)) exhibited only a broad desorption peak at 260, 243, and 219°C, indicating that these catalysts have predominantly weak acidic sites.

Zuo et al. [30] found that, for 7% by weight of Ni/ $\gamma$ -Al<sub>2</sub>O<sub>3</sub>, two broad peaks of NH<sub>3</sub> desorption at approximately 242 and 334°C were attributed to the weak and medium acid sites, respectively. For the HY zeolite-based catalyst, the NH<sub>3</sub> desorption peak was observed at approximately 229°C with a small additional protrusion at 522°C, showing that both weak and strong acidic sites appeared with soft acidity. Menezes et al. [25] found for the CoAl and CoNbAl catalysts that ammonia is desorbed in the range of 100°C to 550°C, and the maximum peaks are located at approximately 280 and 240°C, respectively, indicating that the weak acid sites are predominant in these catalysts. CoNb catalyst showed a sharp peak at 510°C, indicating that this catalyst has predominantly strong acid sites.

### 3.1.6. Fourier-Transform Infrared (FTIR) Spectroscopy.

Figure 7 shows the pyridine-FTIR of all catalysts to perform a qualitative comparison of acid site nature. For the Ni/Al<sub>2</sub>O<sub>3</sub> catalyst, only two bands were observed at 1447 and 1591 cm<sup>-1</sup> which can be attributed to the Lewis acid sites, not the improvised sites found by Brönsted, since no band was noticed between the dates equivalent to these suitable sites.

TABLE 3: Amount of NH<sub>3</sub> desorbed.

Catalyst	NH <sub>3</sub> ( $\mu\text{mol}_{\text{NH}_3}/\text{g}_{\text{cat}}$ )	Ratio acid site (%)		
		Weak	Medium	Strong
Ni/Al <sub>2</sub> O <sub>3</sub>	11.7	19.2	76.5	4.4
Ni/Nb <sub>2</sub> O <sub>5</sub>	10.3	78.3	13.4	8.2
Ni/Beta	42.0	87.3	0.0	12.7
Ni/HY	53.8	48.2	51.8	0.0

Three bands were observed for the Ni/Nb<sub>2</sub>O<sub>5</sub> catalyst at 1447, 1489, and 1606 cm<sup>-1</sup>. The first band (1447 cm<sup>-1</sup>) can be attributed to the Lewis acid sites, the second band (1489 cm<sup>-1</sup>) can be attributed to Lewis and Brönsted acid sites, and the third band (1606 cm<sup>-1</sup>) can be attributed to the Brönsted acid sites [20, 25].

Niobia catalysts have acidic sites for both Brönsted and Lewis. The catalysts containing alumina have only Lewis acidic sites [25]. From the analysis of these data, it was possible to observe that the Nb<sub>2</sub>O<sub>5</sub> catalysts have Lewis and Brönsted acid sites [36, 39]. However, according to Leal et al. [36], from the relative intensities of pyridine adsorbed on the Lewis and Brönsted acid sites, it is possible to conclude that the Brönsted acidity decreases as the Ni loading increases. This characteristic was explained through the ionic exchange of Brönsted acid sites by positively charged Ni species. Still, the authors showed that, for the catalyst containing 25%Ni/Nb<sub>2</sub>O<sub>5</sub>, the support had residual Brönsted acidity and that Lewis acidity was preserved even with the increase of Ni in Nb<sub>2</sub>O<sub>5</sub>.

Meanwhile, for the other catalysts (Ni/Beta and Ni/HY), the bands equivalent to Lewis acid sites appear at 1447 and 1596 cm<sup>-1</sup> (Ni/Beta) and 1447 and 1595 cm<sup>-1</sup> (Ni/HY). Only one band attributed to pyridine adsorbed on Brönsted acid sites appears at 1543 cm<sup>-1</sup> to Ni/Beta, as well as two bands to Ni/HY at 1542 and 1607 cm<sup>-1</sup>. Moreover, the bands at 1491 and 1490 cm<sup>-1</sup> may be due to the pyridine adsorbed at the

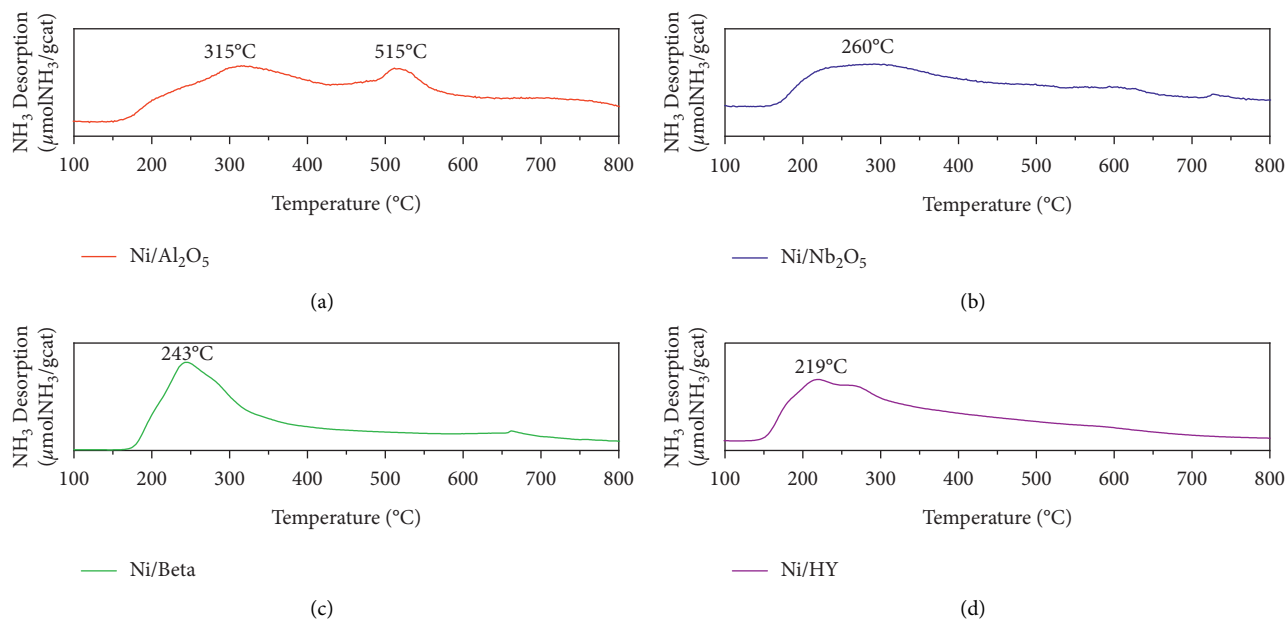


FIGURE 6:  $\text{NH}_3$ -TPD profile of the  $\text{Ni}/\text{Al}_2\text{O}_3$ ,  $\text{Ni}/\text{Nb}_2\text{O}_5$ ,  $\text{Ni}/\text{Beta}$ , and  $\text{Ni}/\text{HY}$  catalysts.

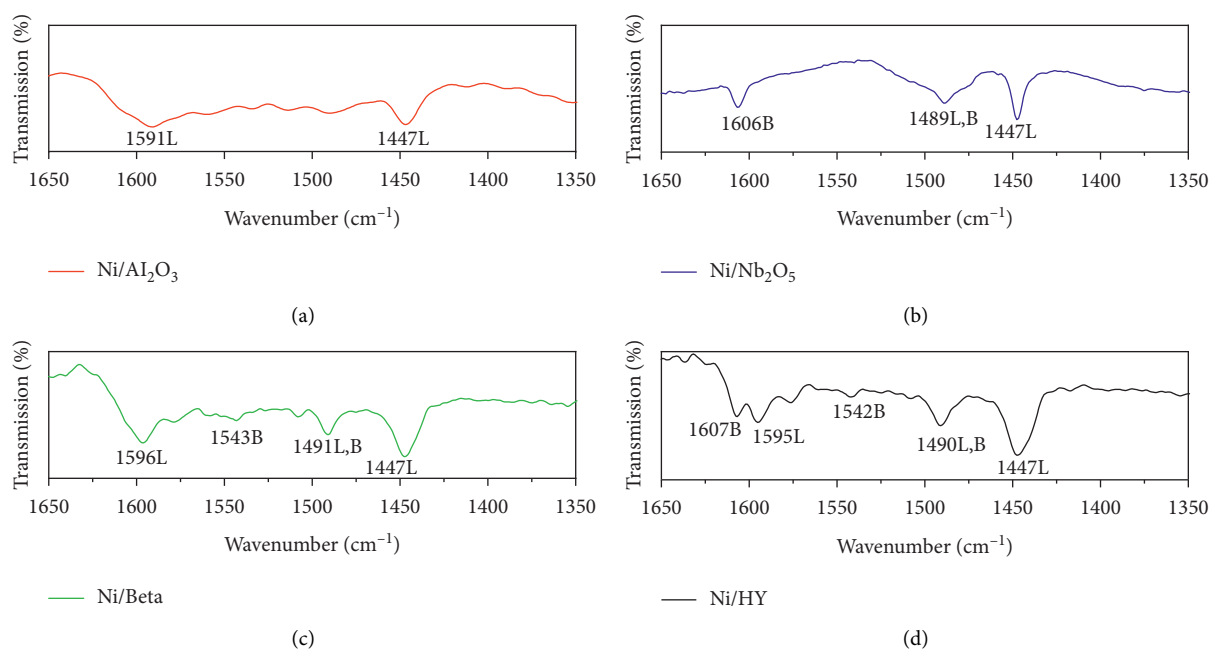


FIGURE 7: Pyridine-FTIR of the  $\text{Al}_2\text{O}_3$ ,  $\text{Ni}/\text{Nb}_2\text{O}_5$ ,  $\text{Ni}/\text{Beta}$ , and  $\text{Ni}/\text{HY}$  catalysts.

Brönsted and Lewis acid sites for the  $\text{Ni}/\text{Beta}$  and  $\text{Ni}/\text{HY}$  catalysts, respectively [37]. Pan et al. [37] found that catalysts containing HY zeolite predominantly present a more significant amount of Brönsted acid sites than Lewis.

Making a comparative analysis, the catalysts containing zeolites clearly showed peaks that are more intense compared to the catalysts comprising oxides. Based on the results, Lewis acidic sites were predominant in all catalysts. When comparing the Lewis peak intensities, it was observed that the  $\text{Ni}/\text{Beta}$  and  $\text{Ni}/\text{HY}$  catalysts showed broader peaks than  $\text{Ni}/\text{Al}_2\text{O}_3$  and  $\text{Ni}/\text{Nb}_2\text{O}_5$  catalysts. In summary, in the

$\text{Ni}/\text{Beta}$  and  $\text{Ni}/\text{HY}$  catalysts, there was a more excellent dispersion of metallic Ni favoring contact with highly dispersed acidic sites in zeolites [40].

**3.2. Catalyst Activity.** The samples were quantified using commercial standards (C10 to C18 hydrocarbons, fatty acids, wax esters, and esters); a standard calibration curve was constructed to identify the reactions' compounds. As predicted, the raw materials were converted into fatty alcohols, fatty acids, wax esters, and hydrocarbons. In the

chromatograms, it was possible to notice some peaks referring to the unconverted esters due to unreacted raw material. The raw materials used in this study are mainly composed of C16 and C18. Consequently, the resulting products are within the range between C9 and C18 due to hydrocracking. Odd carbon chains' predominance was evaluated, with a more significant amount of C15 and C17 hydrocarbons in the samples where Ni/Al<sub>2</sub>O<sub>3</sub> and Ni/Nb<sub>2</sub>O<sub>5</sub> catalysts were used. In contrast, in the samples using Ni/Beta and Ni/HY catalysts, there was a predominance of even carbon chains C16 and C18. This behavior is attributed to hydrodeoxygenation reactions, or decarboxylation/decarbonylation is strongly dependent on the nature of the catalyst, raw material, temperature, and reaction pressure [7, 41].

When analyzing the production of renewable liquid alkanes under standard hydrotreatment conditions (300–450°C), Huber et al. [10] explained that n-C17 hydrocarbons were products of decarbonylation and decarboxylation, while n-C18 was a hydrodeoxygenation product and that the selectivity for decarbonylation and decarboxylation products increases when compared to the hydrodeoxygenation pathway, with the increase in temperature. These results are corroborated by Kiatkittipong et al. [8], who produced a more significant amount of C17 hydrocarbons, justifying that the decarbonylation/decarboxylation reactions were superior to hydrodeoxygenation [42, 43]. These catalysts' metallic and acidic functionalities are responsible for the synergistic effect on hydrodeoxygenation, achieving high FAME conversion and C16 and C18 liquid alkane yields.

In another work [7] on hydroprocessing of crude palm oil, this process's products consisted mainly of n-paraffin (C15–C18). On the other hand, at lower pressures, the hydrodeoxygenation reaction could not be fully achieved, with the appearance of intermediate products, such as fatty alcohols (C16–C18) and esters (C16–C18). Kantama et al. [44] produced naphtha (C5–C8), kerosene (C9–C14), and diesel (C15–C18) and reported the presence of unreacted raw material through the hydroprocessing of fatty acids.

**3.2.1. Total Reagent Conversion and Selectivities.** When analyzing the results, the temperature and reaction time variables, regardless of raw material, were significant for the more excellent conversion of hydrocarbons [26]. The synthesized catalysts promoted the production of hydrocarbons in the lowest reaction conditions but lower proportions.

Table 4 presents the percentage areas of hydrocarbons produced in all reaction conditions for the different catalysts based on oxides.

Table 4 shows that the catalysts showed good conversion for the two raw materials used. Niobia has lesser acidity than alumina, according to the TPD analysis, which may explain the reason for the minimized hydrocarbon and cracking reactions [27, 45, 46].

According to Peng et al. [47], the data obtained through NH<sub>3</sub>-TPD for nickel catalysts, including for those

supported on  $\gamma$ -Al<sub>2</sub>O<sub>3</sub>, showed that the effect of the support is related to the acidic sites developed on the surface which can catalyze dehydration reactions and thus facilitate the formation of alkanes through hydrogenation by the nickel-metal sites. Also, according to these authors, some complete conversions to n-alkanes observed for catalysts such as Ni/Beta were attributed to the Brønsted acid sites developed on the surface, favoring hydroisomerization and hydrocracking, in contrast to those supported on oxides that present mainly Lewis and Brønsted acid sites [47].

The best selectivities of hydrocarbons were obtained at temperature and time's most significant reaction conditions. The low selectivity presented by the Niobia catalyst with palm oil may be related to the instability of this catalyst in the presence of by-products such as water and CO<sub>x</sub>, resulting from the decarboxylation/decarbonylation reactions that occur during the conversion of triglycerides [48].

Niobia has a strong metal-support interaction (SMSI), which explains the migration of reduced species from the support to the surface of metal particles which can be influenced by high reduction temperatures [48, 49]. However, this migration of the mobile phase can cause the decrease of the available metallic surface and start the formation of the interface between the metal and the oxide, which may be the factor responsible for the significant difference in the catalyst activity [50]. This effect causes the appearance of new active acidic sites on the surface, which can influence the activity and selectivity in reactions sensible to the fresh catalyst structure [51, 52]. Studies show that Nb<sub>2</sub>O<sub>5</sub> as a support is a reducible oxide and interacts with the active phase, affecting the structure and interface of the metal. Through characterization techniques such as XRD, it is possible to observe the effect of this strong metal-support interaction (SMSI) [31].

The high hydrocarbon yield shown for Ni/Al<sub>2</sub>O<sub>3</sub> can be attributed to pure nickel in contact with the surface of alumina, which exhibits an increase in total acidity, mainly increasing the number of medium and strong acidic sites, consequently providing a high surface area. Similar results were found by Gousi et al. [26], who demonstrated that the reagent conversion and the total yield of hydrocarbons increase over time, while the yield of intermediate products initially increases and then decreases. Also, others reported that selectivity could also increase or decrease according to the nickel content in the catalyst. Depending on the percentage (above 60%), there may be a drastic decrease in the specific surface area, preventing achieving a high active surface [26].

The best selectivity at optimum conditions was justified and discussed by Rocha et al. [12], who reported that high reaction conditions are necessary for the more excellent conversion of reagents into hydrocarbons from triglycerides. The most significant amount of these hydrocarbons was C17 due to decarbonylation/decarboxylation reactions.

Through the analysis of Table 4, it was noticeable that oils have less selectivity about esters. Unsaturated compounds in the oil can cause the catalyst to be deactivated and, consequently, reduce catalytic activity, presenting a lower

TABLE 4: Conversion of reagents (palm oil; soy methyl ester) and hydrocarbons selectivity in catalytic hydroprocessing.

Time (h)	Temp (°C)	Palm oil						Soy methyl ester								
		Ni/Al <sub>2</sub> O <sub>3</sub> Selectivity (%)			Ni/Nb <sub>2</sub> O <sub>5</sub> Selectivity (%)			Ni/Al <sub>2</sub> O <sub>3</sub> Selectivity (%)			Ni/Nb <sub>2</sub> O <sub>5</sub> Selectivity (%)					
		Conv. (%)	HC	Fatty acids	Wax esters	Fatty alcohols	Conv. (%)	HC	Fatty acids	Wax esters	Fatty alcohols	Conv. (%)	HC	Fatty acids	Wax esters	Fatty alcohols
5	270	100	6.0	37.1	54.3	2.6	100	1.1	42.5	10.1	46.3	53.3	4.4	46.7	48.0	0.9
	290	100	11.0	49.5	36.7	2.4	100	0.9	71.6	6.0	21.5	59.4	24.3	40.6	34.4	0.7
	300	100	22.6	51.6	24.8	0.9	100	0.2	85.4	2.0	12.3	50.1	29.9	49.9	19.5	0.7
7	270	100	8.1	40.4	49.4	2.1	100	1.5	46.6	14.3	37.6	61.1	7.9	38.9	52.2	1.0
	290	100	23.8	35.4	38.3	2.1	100	0.9	78.7	5.9	14.5	55.3	29.5	44.7	25.2	0.6
	300	100	21.0	58.1	20.2	0.7	100	1.1	79.2	7.1	12.6	98.3	41.2	41.9	16.1	0.8

selectivity for hydrocarbons. The catalytic activity and selectivity of products for hydroprocessing depend strongly on the acidity of the supports [53]. However, the catalytic hydroprocessing of triglycerides presents the disadvantage of low efficiency of liquid fuels and enormous loss of carbon in gaseous products. The hydrodeoxygenation of fatty acids, similar to the technology existing in oil refineries, is another promising technology for producing high-performance liquid fuels.

Kiatkittipong et al. [8] produced hydrocarbons in the range of petroleum diesel through catalytic hydroprocessing to evaluate the effects of operational parameters and catalyst types to determine each raw's appropriate conditions material, using crude and refined palm oil and palm fatty acids. The authors found that the hydroprocessing of crude palm oil (400°C, 40 bar, and a reaction time of 3 hours) showed a 51% hydrocarbon yield. In the analysis carried out for refined palm oil, the yield reached 70%, with a shorter reaction time (1 hour). In the study performed for the hydroprocessing of fatty acids, a higher hydrocarbon yield was observed in less severe conditions (375°C and reaction time of 30 minutes), reaching 81%.

Given these facts, it is evident that the hydroprocessing of fatty acids to produce hydrocarbons in the diesel range is more efficient than triglycerides, since the fatty acid compositions are mainly free fatty acids (palmitic, oleic, and linoleic), which can be easily converted to aliphatic alkanes when compared to triglycerides.

The evaluation of the activity of the zeolite-supported catalysts in the conversion of the methyl ester of soy and fatty acids during hydroprocessing and selectivity for hydrocarbons can be seen in Table 5.

In these catalysts, temperature and reaction time were increased to 340°C and 9 hours to evaluate the effect of temperature and time.

In the reactions using ester as raw material, at the highest temperature (340°C) and time (9 hours) conditions for the Ni/Beta catalyst (76.8%) verified significant activity. The selectivity was lower for the reaction catalyzed with Ni/HY (61.9%) in the same reaction condition. However, for a lower temperature (300°C), the reaction performed with the Ni/HY catalyst obtained more selectivity for 9 h, reaching a percentage of 81.2%.

The results indicate that the reaction favors the formation of fatty acids at high temperatures for the Ni/HY catalyst. For Ni/Beta, the situation is the opposite; the lower the temperature, the higher the production of fatty acids. According to TPD, Beta has more strong acid sites (Brønsted), so it has higher activity and somehow avoids the formation of fatty acids, which is the principal intermediate in this reaction. The decrease in Ni/HY activity with increasing temperature and time may be related to the blocking of pores by the nickel particles in the support, resulting from the sintering process that can occur during the preparation of the catalyst [54].

Both catalysts had maximum selectivity (100%) for the reaction condition at 340°C and 9 hours in the hydroprocessing of fatty acids. The hydrocarbons increased with increasing temperature and reaction time for both catalysts.

In general, the results showed that both catalysts have good catalytic activity, with very close values. The high selectivity obtained can be explained due to these catalysts' metallic and acid functionalities in the hydrotreating of fatty acids [6].

The influence of the support and its acidic properties can discuss several concepts. There may be an influence on activity and selectivity motivated by the acidity of the support and, consequently, a change in the catalyst structure. Optionally, acidic sites can be directly involved in the reactions [9, 30]. A possible explanation for this high selectivity may be related to the sequential hydrogenation of fatty acids to aldehydes and fatty alcohols on the nickel-metal surface, followed by the dehydration of fatty alcohols, at the Brønsted acid sites in olefins and in the hydrogenation of the double bond of the metal [9].

Based on the results in Table 5, in the reactions with ester as raw material, zeolite as support showed conversion in the highest temperature (340°C) and time (9 h), reaching 99.1% for Beta zeolite and 100% for HY. Besides, in milder conditions, zeolites also promoted the conversion of reagents but in a slightly lower percentage, between 82-99% for the ester. Based on TPD and FTIR, the more excellent conversion and selectivity shown by the catalyst supported in Beta can be attributed to the catalyst's greater surface area and acidity.

In the reactions with fatty acids, conversions of less than 71.1 and 63.5% were obtained for the Beta and HY zeolites, correspondingly, in the most extreme reaction conditions. This characteristic is linked to unsaturated compounds in the raw material that can cause the catalyst to be deactivated, reduce catalytic activity, and show less conversion. To maximize the reagent conversion, some authors even use technologies to convert lipid raw materials into distillate fuels [9]. In this context, an optimum acidity value of the substrate allows relatively high activity and low cracking or imperfections on the catalyst's surface. Another factor related to good performance was that the particle size of the nickel or nickel oxide detected by the XRD was minimal, indicating that the species were highly dispersed on the surface of the supports [30].

Catalysts based on zeolites favored hydrocracking, with low selectivity for C15 and C16 alkanes [30]. The most promising catalysts for this work were Ni/ $\gamma$ -Al<sub>2</sub>O<sub>3</sub> and Ni/SAPO-11, which showed high activity and selectivity for these alkanes' production. This good catalytic performance was attributed to the acidity of the catalysts. In this context, an optimum acidity value in the substrates allows obtaining relatively high activity and low cracking or imperfections on the catalysts' surface. Another factor related to good performance was that the particle size of the nickel or nickel oxide detected by the DRX was minimal, indicating that the species were highly dispersed on the supports' surface [30].

Analyzing the conversion of intermediate products under lower reaction conditions found a higher percentage. According to Guzman et al. [7], these compounds are most likely formed by thermal decomposition and can be produced from a molecule of triglyceride, aldehyde, or long-chain alcohols. Therefore, it is assumed that the observed high molecular weight esters (wax esters) result from the

TABLE 5: Conversion of reagents (soy methyl ester; fatty acids) and hydrocarbons selectivity in catalytic hydroprocessing.

Time (h)	Temp. (°C)	Soy methyl ester						Fatty acids											
		Ni/Beta			Ni/HY			Ni/Beta			Ni/HY								
		Conversion (%)	HC Selectivity (%)	Fatty acids	Wax esters	Conversion (%)	HC Selectivity (%)	Fatty acids	Wax esters	Conversion (%)	HC Selectivity (%)	Fatty acids	Wax esters	Conversion (%)	HC Selectivity (%)	Fatty acids	Wax esters	alcohols	
7	300	99	30.3	67.9	1.8	99	73.0	23.0	0	32	97.5	0	2.5	0	18	88.5	0	0	11.5
	340	99	72.9	27.1	0	100	58.4	41.6	0	70	99.0	0	0	0	57	95.4	0	4.6	0
9	300	90	70.7	29.3	0	99	81.2	18.8	0	39	97.4	0	2.6	0	30	94.3	0	1.7	4
	340	99	76.8	23.2	0	100	61.9	38.1	0	71	100	0	0	0	63	100	0	0	0

reaction between a fatty acid and long-chain alcohol, which are the possible intermediate products of the reactions involved in this process.

According to data that has been reported in the literature, the highest yields of intermediate products are achieved under milder temperature and pressure conditions. Hydroprocessing should be carried out under conditions that do not favor the formation of these coproducts, using temperatures above 350°C. Therefore, by increasing the reaction conditions, it is possible to increase the hydrogenation of wax esters and the dehydration/hydrogenation of fatty alcohols and thus increase the production of hydrocarbons [10]. Furthermore, most reactions are carried out with the addition of some organic solvents to ensure more excellent conversion and selectivity [55–57]. Wax esters are considered the most stable intermediate product of the process. These by-products are transformed into fatty alcohols through hydrogenation, a slower and determining step in the reaction [39].

According to the literature, the main intermediate products resulting from the deoxygenation of vegetable oils and derivatives are acids, aldehydes, and alcohol. The generation and consumption rates are the determining factors for the total deoxygenation capacity and selectivity. Given this fact, the importance of studying reaction kinetics to determine the concentrations of each reaction product emerges [58].

Other studies have shown the complexity and variety of intermediate products resulting from hydroprocessing, including alcohols, acids, esters, aldehydes, and ketones, causing difficulties in analyzing the exact composition and understanding the reaction pathways. With the proposal of an efficient method of analysis of four-dimensional gas chromatography combined with mass spectrometry (GC × GC-TOFMS), Kim et al. [59] understood that different reaction pathways arise when other catalysts appear and reaction conditions are used. In general, Ni catalysts tend to activate decarboxylation and decarbonylation reactions.

The results showed that it is possible to hydrogenate triglycerides and derivatives to transform them into hydrocarbons. Also, the appropriate choice of operational parameters and raw materials influences hydrocarbons' conversion and selectivity. Esters were more easily converted, and fatty acids were more efficient for selectivity. Oxide-based catalysts showed good catalytic activity; however, they were more sensitive to reaction factors. In contrast, zeolites showed excellent catalytic activity, a factor related to the high acidity of Brønsted present in these catalysts.

#### 4. Conclusions

In this scenario, the evidence from this study suggests that the production of hydrocarbons should be based on the type of raw material, catalyst pretreatment, and reaction conditions. In general, this work revealed that catalysts with a more significant number of acidic Brønsted sites and greater surface area and pore volume showed better catalytic performance, resulting in milder reaction conditions during hydroprocessing, allowing a reduction time of 5 hours, which provide more significant energy savings.

Furthermore, the conversion of reagents to distillate fuels can maximize the production of hydrocarbons. The hydroprocessing reaction of palm oil, soybean methyl ester, and fatty acids catalyzed on oxides and zeolites supported on nickel showed satisfactory results under the conditions studied for the production of hydrocarbons. The greatest selectivities were observed through the hydroprocessing of soybean methyl ester when using the Ni/Al<sub>2</sub>O<sub>3</sub> catalyst (41.2%) and the hydroprocessing of fatty acids when using the zeolites Beta and HY, both 100%. The increase in reaction time and temperature improved the conversion of hydrocarbons. Given the excellent performance of catalysts in the catalytic hydroprocessing reaction compared to conversions conducted with noble metals commonly used in the biofuel industry, it is possible to consider them as promising alternative routes, as the application of transition metals as a catalyst will reduce the production cost.

#### Data Availability

The data used to support the findings of this study are included within the article.

#### Conflicts of Interest

The authors declare that there are no conflicts of interest regarding the publication of this paper.

#### Acknowledgments

The authors thank Coordenação de Aperfeiçoamento de Pessoal de Nível Superior (CAPES) and INCT-MIDAS from Science and Technology Ministry-Brazil for their financial support.

#### References

- [1] Anac, *Brazil's Action Plan on CO<sub>2</sub> Emissions Reduction from Aviation*, 2018.
- [2] I. A. T. A. IATA, *Annual Review*, 2018.
- [3] D. Chiaramonti, M. Prussi, M. Buffi, and D. Tacconi, "Sustainable bio kerosene: process routes and industrial demonstration activities in aviation Biofuels," *Applied Energy*, vol. 136, pp. 767–774, 2014.
- [4] A. Llamas, M. J. García-Martínez, A.-M. Al-Lal, L. Canoira, and M. Lapuerta, "Biokerosene from coconut and palm kernel oils: production and properties of their blends with fossil kerosene," *Fuel*, vol. 102, pp. 483–490, 2012.
- [5] D. Kubička, P. Simacek, and N. Zilkova, "Transformation of vegetable oils into hydrocarbons over mesoporous-alumina-supported CoMo catalysts," *Topics in Catalysis*, vol. 52, pp. 161–168, 2009.
- [6] L. Chen, H. Li, J. Fu, C. Miao, P. Lv, and Z. Yuan, "Catalytic hydroprocessing of fatty acid methyl esters to renewable alkane fuels over Ni/HZSM-5 catalyst," *Catalysis Today*, vol. 259, pp. 266–276, 2016.
- [7] A. Guzman, J. E. Torresuan, L. P. Prada, and M. L. Nuñez, "Hydroprocessing of crude palm oil at pilot plant scale. Catal," *Catalysis Today*, vol. 156, no. 25, pp. 38–43, 2010.
- [8] W. Kiatkittipong, S. Phimsen, K. Kiatkittipong, S. Wongsakulphasatch, N. Laosiripojana, and S. Assabumrungrat, "Diesel-like hydrocarbon production

- from hydroprocessing of relevant refining palm oil," *Fuel Processing Technology*, vol. 116, pp. 16–26, 2013.
- [9] I. Hachemi, N. Kumar, P. Mäki-Arvela et al., "Sulfur-free Ni catalyst for production of green diesel by hydrodeoxygenation," *Journal of Catalysis*, vol. 347, pp. 205–221, 2017.
- [10] G. W. Huber, P. O'Connor, and A. Corma, "Processing biomass in conventional oil refineries: production of high quality diesel by hydrotreating vegetable oils in heavy vacuum oil mixtures," *Applied Catalysis A: General*, vol. 329, pp. 120–129, 2007.
- [11] K. Pongsiriyakul, W. Kiatkittipong, K. Kiatkittipong et al., "Alternative hydrocarbon biofuel production via hydro-treating under synthesis gas atmosphere," *Energy & Fuels*, vol. 31, no. 11, pp. 12256–12262, 2017.
- [12] A. Rocha, A. Farojr, L. Oliviero, J. Vangestel, and F. Mauge, "Alumina-, niobia, and niobia/alumina supported NiMoS catalysts: surface properties and activities in the hydrodesulfurization of thiophene and hydrodenitrogenation of 2,6-dimethylaniline," *Journal of Catalysis*, vol. 252, no. 2, pp. 321–334, 2007.
- [13] B. C. Klein, M. F. Chagas, T. L. Junqueira et al., "Techno-economic and environmental assessment of renewable jet fuel production in integrated Brazilian sugarcane biorefineries," *Applied Energy*, vol. 209, pp. 290–305, 2018.
- [14] C. M. Alves, S. de Jong, A. Bonomi, L. A. M. van der Wielen, and S. I. Mussatto, "Techno-economic assessment of biorefinery technologies for aviation biofuels supply chains in Brazil," *Biofuels, Bioproducts and Biorefining*, vol. 11, no. 1, pp. 67–91, 2017.
- [15] W.-C. Wang and L. Tao, "Bio-jet fuel conversion technologies," *Renewable and Sustainable Energy Reviews*, vol. 53, pp. 801–822, 2016.
- [16] R. Mawhood, E. Gazis, S. de Jong, R. Hoefnagels, and R. Slade, "Production pathways for renewable jet fuel: a review of commercialization status and future prospects," *Biofuels, Bioproducts and Biorefining*, vol. 10, no. 4, pp. 462–484, 2016.
- [17] R. Kumar, B. S. Rana, R. Tiwari et al., "Hydroprocessing of jatropha oil and its mixtures with gas oil," *Green Chemistry*, vol. 12, no. 12, pp. 2232–2239, 2010.
- [18] C. Gutiérrez-Antonio, F. I. Gómez-Castro, J. A. Lira-Flores, and S. Hernández, "A review on the production processes of renewable jet fuel," *Renewable and Sustainable Energy Reviews*, vol. 79, pp. 709–729, 2017.
- [19] I. Kubicková, M. Snare, K. Eranen, Maki-Arvela, and D. Y. Murzin, "Hydrocarbons for diesel fuel via decarboxylation of vegetable oils," *Catalysis Today*, vol. 106, pp. 197–200, 2005.
- [20] L. Chen, J. Fu, L. Yang, Z. Chen, Z. Yuan, and P. Lv, "Catalytic hydrotreatment of fatty acid methyl esters to diesel-like alkanes over hb zeolite-supported nickel," *ChemCatChem*, vol. 6, no. 12, pp. 3482–3492, 2014.
- [21] A. Galadima and Muraza, "Catalytic upgrading of vegetable oils into jet fuels range hydrocarbons using heterogeneous catalysts: a review," *Journal of Industrial and Engineering Chemistry*, vol. 29, pp. 12–23, 2015.
- [22] M. Schmal, "Catalise heterogênea," in *Synergia, 1°*, pp. 1–376, Rio de Janeiro, 2011.
- [23] K. V. R. Chary, P. V. R. Rao, K. S. R. Rao, and M. Papadaki, "Characterization and catalytic properties of niobia supported nickel catalysts in the hydrodechlorination of 1, 2, 4-trichlorobenzene," *Journal of Molecular Catalysis A: Chemical*, vol. 223, no. 1-2, pp. 353–361, 2004.
- [24] Y. Liu, K. Murata, T. Minowa, and K. Sakanishi, "Hydro-treatment of vegetable oil to produce bio-hydrogenated diesel and liquefied petroleum gas fuel over catalysts containing sulfided Ni-Mo and solid acids," *Energy & Fuels*, vol. 25, no. 10, pp. 4675–4685, 2011.
- [25] J. P. d. S. Q. Menezes, K. R. Duarte, R. L. Manfro, and M. M. V. M. Souza, "Effect of niobia addition on cobalt catalysts supported on alumina for glycerol steam reforming," *Renewable Energy*, vol. 148, pp. 864–875, 2020.
- [26] M. Gousi, C. Andriopoulou, K. Bourikas et al., "Green diesel production over nickel-alumina co-precipitated catalysts," *Applied Catalysis A: General*, vol. 536, pp. 45–56, 2017.
- [27] R. J. da Silva, A. F. Pimentel, R. S. Monteiro, and C. J. A. Mota, "Synthesis of methanol and dimethyl ether from the CO<sub>2</sub> hydrogenation over Cu•ZnO supported on Al<sub>2</sub>O<sub>3</sub> and Nb<sub>2</sub>O<sub>5</sub>," *Journal of CO<sub>2</sub> Utilization*, vol. 15, pp. 83–88, 2016.
- [28] L. P. C. Silva, M. M. Freitas, R. M. Santos et al., "The effect of metal type on the sulfur tolerance of catalysts supported on niobia for sour water-gas shift reaction," *International Journal of Hydrogen Energy*, vol. 43, no. 6, pp. 3190–3202, 2018.
- [29] I.-H. Choi, K.-R. Hwang, J.-S. Han, K.-H. Lee, J. S. Yun, and J.-S. Lee, "The direct production of jet-fuel from non-edible oil in a single-step process," *Fuel*, vol. 158, pp. 98–104, 2015.
- [30] H. Zuo, Q. Liu, T. Wang, L. Ma, Q. Zhang, and Q. Zhang, "Hydrodeoxygenation of methyl palmitate over supported ni catalysts for diesel-like fuel production," *Energy & Fuels*, vol. 26, no. 6, pp. 3747–3755, 2012.
- [31] L. F. d. Sousa, S. M. Landi, and M. Schmal, "Investigation of structures and metallic environment of the Ni/Nb<sub>2</sub>O<sub>5</sub> by different in situ treatments – effect on the partial oxidation of methane," *Applied Catalysis A: General*, vol. 537, pp. 100–110, 2017.
- [32] A. Quindimil, U. De-La-Torre, B. Pereda-Ayo, J. A. González-Marcos, and J. R. González-Velasco, "Ni catalysts with La as promoter supported over Y- and BETA- zeolites for CO<sub>2</sub> methanation," *Applied Catalysis B: Environmental*, vol. 238, pp. 393–403, 2018.
- [33] P. Prieceľ, D. Kubička, L. Čapek, Z. Bastl, and P. Ryšánek, "The role of Ni species in the deoxygenation of rapeseed oil over NiMo-alumina catalysts," *Applied Catalysis A: General*, vol. 397, no. 1-2, pp. 127–137, 2011.
- [34] J. Horáček, Z. Tišler, V. Rubáš, and D. Kubicka, "HDO catalysts for triglycerides conversion into pyrolysis and isomerization feedstock," *Fuel*, vol. 121, pp. 54–67, 2014.
- [35] A. Srifa, K. Faungnawakij, V. Itthibenchapong, and S. Assabumrungrat, "Roles of monometallic catalysts in hydrodeoxygenation of palm oil to green diesel," *Chemical Engineering Journal*, vol. 278, pp. 249–258, 2015.
- [36] G. F. Leal, S. Lima, I. Graça et al., "Design of nickel supported on water-tolerant Nb<sub>2</sub>O<sub>5</sub> catalysts for the hydrotreating of lignin streams obtained from lignin-first biorefining," *iScience*, vol. 15, pp. 467–488, 2019.
- [37] Z. Pan, R. Wang, and J. Chena, "Catalytic deoxygenation of methyl laurate as a model compound to hydrocarbons on hybrid catalysts composed of Ni-Zn alloy and HY zeolite," *Journal of Chemical Technology & Biotechnology*, vol. 94, pp. 3007–3019, 2019.
- [38] N. Shi, Q.-y. Liu, T. Jiang et al., "Hydrodeoxygenation of vegetable oils to liquid alkane fuels over Ni/HZSM-5 catalysts: methyl hexadecanoate as the model compound," *Catalysis Communications*, vol. 20, pp. 80–84, 2012.
- [39] G. J. Muchave, L. D. S. Netto, J. M. A. R. Almeida, and D. A. G. Aranda, "Synthesis of fatty alcohols by hydrogenation of palm esters using rhenium-based catalysts supported on

- niobia, alumina and titania,” *International Journal of Development Research*, vol. 10, no. 11, pp. 42266–42278, 2020.
- [40] E. M. Thyssen, V. V. Maia, and T. A. Assaf, “Cu and Ni catalysts supported on  $\gamma$ -Al<sub>2</sub>O<sub>3</sub> and SiO<sub>2</sub> assessed in glycerol steam reforming reaction,” *Journal of the Brazilian Chemical Society*, vol. 26, pp. 22–31, 2015.
- [41] V. A. Yakovlev, S. A. Khromova, O. V. Sherstyuk et al., “Development of new catalytic systems for upgraded bio-fuels production from bio-crude-oil and biodiesel. Catal,” *Catalysis Today*, vol. 144, no. 3–4, pp. 362–366, 2009.
- [42] S. Phimsen, W. Kiatkittipong, H. Yamada et al., “Oil extracted from spent coffee grounds for bio-hydrotreated diesel production,” *Energy Conversion and Management*, vol. 126, pp. 1028–1036, 2016.
- [43] S. Phimsen, W. Kiatkittipong, H. Yamada et al., “Nickel sulfide, nickel phosphide and nickel carbide catalysts for biohydrotreated fuel production,” *Energy Conversion and Management*, vol. 151, pp. 324–333, 2017.
- [44] A. Kantama, P. Narataruksa, P. Hunpinyo, and C. Prapainainar, “Techno-economic assessment of a heat-integrated process for hydrogenated renewable diesel production from palm fatty acid distillate,” *Biomass and Bioenergy*, vol. 83, pp. 448–459, 2015.
- [45] A. C. Faro Jr, P. Grange, and A. C. B. dos Santos, “Niobia-supported nickel–molybdenum catalysts: characterisation of the oxide form,” *Physical Chemistry Chemical Physics*, vol. 4, no. 16, pp. 3997–4007, 2002.
- [46] A. Faro Jr and A. Dossantos, “Cumene hydrocracking and thiophene HDS on niobia-supported Ni, Mo and Ni–Mo catalysts,” *Catalysis Today*, vol. 118, no. 3–4, pp. 402–409, 2006.
- [47] B. Peng, C. Zhao, S. Kasakov, S. Foraita, and J. A. Lercher, “Manipulating catalytic pathways: deoxygenation of palmitic acid on multifunctional catalysts,” *Chemistry - A European Journal*, vol. 19, no. 15, pp. 4732–4741, 2013.
- [48] A. Jasik, R. Wojcieszak, S. Monteverdi, M. Ziolek, and M. M. Bettahar, “Study of nickel catalysts supported on Al<sub>2</sub>O<sub>3</sub>, SiO<sub>2</sub> or Nb<sub>2</sub>O<sub>5</sub> oxides,” *Journal of Molecular Catalysis A: Chemical*, vol. 242, no. 1–2, pp. 81–90, 2005.
- [49] R. Wojcieszak, A. Jasik, S. Monteverdi, M. Ziolek, and M. M. Bettahar, “Nickel niobia interaction in non-classical Ni/Nb<sub>2</sub>O<sub>5</sub> catalysts,” *Journal of Molecular Catalysis A: Chemical*, vol. 256, no. 1–2, pp. 225–233, 2006.
- [50] J. Li, G. Lu, K. Li, and W. Wang, “Active Nb<sub>2</sub>O<sub>5</sub>-supported nickel and nickel–copper catalysts for methane decomposition to hydrogen and filamentous carbon,” *Journal of Molecular Catalysis A: Chemical*, vol. 221, no. 1–2, pp. 105–112, 2004.
- [51] M. Schmal, D. A. G. Aranda, R. R. Soares, F. B. Noronha, and A. Frydman, “A study of the promoting effect of noble metal addition on niobia and niobia alumina catalysts,” *Catalysis Today*, vol. 57, no. 3–4, pp. 169–176, 2000.
- [52] F. M. T. Mendes, C. A. C. Perez, F. B. Noronha et al., “Fischer–Tropsch synthesis on anchored Co/Nb<sub>2</sub>O<sub>5</sub>/Al<sub>2</sub>O<sub>3</sub> catalysts: the nature of the surface and the effect on chain growth,” *The Journal of Physical Chemistry B*, vol. 110, no. 18, pp. 9155–9163, 2006.
- [53] P. Kumar, S. R. Yenumala, S. K. Maity, and D. Shee, “Kinetics of hydrodeoxygenation of stearic acid using supported nickel catalysts: effects of supports,” *Applied Catalysis A: General*, vol. 471, pp. 28–38, 2014.
- [54] N. Hanif, M. W. Anderson, V. Alfredsson, and O. Terasaki, “The effect of stirring on the synthesis of intergrowths of zeolite Y polymorphs,” *Physical Chemistry Chemical Physics*, vol. 2, no. 14, pp. 3349–3357, 2000.
- [55] E. Furimsky, “Hydroprocessing challenges in biofuels production,” *Catalysis Today*, vol. 217, pp. 13–56, 2013.
- [56] L. Hermida and A. R. Mohamed, “Deoxygenation of fatty acid to produce diesel-like hydrocarbons: a review of process conditions, reaction kinetics and mechanism,” *Renewable and Sustainable Energy Reviews*, vol. 42, pp. 1223–1233, 2015.
- [57] R. D. Pantanaïs and B. P. Misra, “Effect of reaction pathway and operating parameters on the deoxygenation of vegetable oils to produce diesel range hydrocarbon fuels: a review,” *Renewable and Sustainable Energy Reviews*, vol. 73, pp. 545–557, 2017.
- [58] H. Zhang, H. Lin, W. Wang, Y. Zheng, and P. Hu, “Hydroprocessing of waste cooking oil over a dispersed nano catalyst: kinetics study and temperature effect,” *Applied Catalysis B: Environmental*, vol. 150–151, pp. 238–248, 2014.
- [59] S. K. Kim, J. Y. Han, H.-s. Lee, T. Yum, Y. Kim, and J. Kim, “Production of renewable diesel via catalytic deoxygenation of natural triglycerides: comprehensive understanding of reaction intermediates and hydrocarbons,” *Applied Energy*, vol. 116, pp. 199–205, 2014.